

# The Influence of Nonequilibrium Distribution on Room-Temperature Lasing Spectra in Quantum-Dash Lasers

C. L. Tan, *Student Member, IEEE*, H. S. Djie, *Member, IEEE*, Y. Wang, *Student Member, IEEE*, C. E. Dimas, *Student Member, IEEE*, V. Hongpinyo, *Student Member, IEEE*, Y. H. Ding, *Student Member, IEEE*, and B. S. Ooi, *Senior Member, IEEE*

**Abstract**—We demonstrate the effect of nonequilibrium carrier distribution in a self-assembled InAs–InAlGaAs quantum-dash-in-well semiconductor lasers on InP substrate. The progressive changes of electroluminescence spectrum with increasing injections show the presence of localized photon reabsorption and lasing action from different dash ensembles at room temperature as opposed to that obtained in typical self-assembled quantum-dot lasers only at low temperature below 100 K.

**Index Terms**—Nonequilibrium distribution, quantum-dash (Qdash), quantum-dot (QD), supercontinuum broadband laser.

## I. INTRODUCTION

SELF-ASSEMBLY technology has attracted considerable interest in the growth of quantum-dot (QD)/quantum-dash (Qdash) optical amplifiers and semiconductor lasers due to the unprecedented potential offered by the three-dimensional energy levels quantification [1]. In recent years, Qdash lasers have presented their superior performances of lower threshold current, lower chirp, higher gain, and higher thermal stability than the conventional quantum well (QW) or bulk-heterostructure-based photonic devices [1]. Recently, self-assembled QD lasers have been shown to emit unique lasing spectral characteristics, where the laser emission spectra are broadened with modulated nonlasing spectral regions and the number of lasing modes increases above threshold [2]. This unexpected behavior has been attributed to the carrier localization in noninteracting dots and a resultant inhomogeneously broadened gain spectrum. An experimental observation of extraordinary wideband lasing coverage of 50 nm at a low temperature (60 K) from QD laser [3] has been attributed to the nonequilibrium carrier distribution

[4] among self-assembled QD with different sizes and compositions due to the longer carrier emission time. These interesting features of self-organized, spatially isolated nanostructure technology have led to the realization of broad interband semiconductor lasers that can be widely applied in optical telecommunication, various sensors detecting chemical agents, atmospheric or planetary gases, high-precision optical metrology and spectroscopy, biomedical imaging, and pump sources for eye-safe erbium-doped solid-state lasers [5]. In addition, it is natural to expect that narrow pulses can be generated by locking the phases of modes in the supercontinuum broad laser spectrum under mode-locked operation [6] due to the fast carrier dynamics and the broad gain bandwidth [1].

In this letter, we demonstrate the presence of lasing action from different sizes or groups of Qdash ensembles in addition to emission from different excited states within the same Qdash ensemble that shows promise towards realizing supercontinuum broad laser linewidth at room-temperature operation. This is in contrast to prior observation from self-assembled QD lasers that occur only at low temperature below 100 K [3], [4]. The occurrence of photon reabsorption among different sizes of Qdash ensembles contribute to dominant lasing from large sized Qdashes at longer wavelength regime.

## II. EXPERIMENT

The Qdash laser structure was grown by molecular beam epitaxy on (100) oriented InP substrate. The active region consists of four sheets of five monolayers of InAs dashes, each embedded within a 7.6-nm-thick compressively strained  $\text{In}_{0.64}\text{Ga}_{0.16}\text{Al}_{0.2}\text{As}$  QW and a 30-nm-thick tensile strained  $\text{In}_{0.50}\text{Ga}_{0.32}\text{Al}_{0.18}\text{As}$  barrier [5]. A 475-nm layer of  $\text{SiO}_2$  was deposited on samples using plasma-enhanced chemical vapor deposition prior to rapid thermal annealing at 750 °C in a nitrogen ambient for 1 min. Broad-area lasers with 50- $\mu\text{m}$ -wide oxide stripes were fabricated from the intermixed Qdash samples. A fresh 200-nm-thick  $\text{SiO}_2$  layer was deposited and a 50- $\mu\text{m}$  contact window was defined using a 10% buffered oxide etchant. In order to maximize the gain, the optical cavity was aligned along the [011] orientation which is perpendicular to the dash elongation direction. A p-metal contact consisting of Ti–Au layers was defined using electron beam evaporation and liftoff process. The samples were thinned down to  $\sim 150 \mu\text{m}$  and n-metal contact of Au–Ge–Au–Ni–Au layers was evaporated on the back side of the samples. After cleaving the

Manuscript received August 05, 2008; revised October 15, 2008. First published October 31, 2008; current version published January 05, 2009. This work was supported in part by the National Science Foundation (NSF) under Grant 0725647, U.S. Army Research Laboratory, Commonwealth of Pennsylvania, Department of Community and Economic Development.

C. L. Tan, C. E. Dimas, V. Hongpinyo, Y. H. Ding, and B. S. Ooi are with the Center for Optical Technologies and Department of Electrical and Computer Engineering, Lehigh University, Bethlehem, PA 18015 USA (e-mail: bsooi@lehigh.edu).

H. S. Djie was with Lehigh University and is now with the JDS Uniphase Corp., San Jose, California 95134, USA.

Y. Wang was with the Lehigh University, Bethlehem, PA 18015 USA, and is now with the OptiComp Corp., Zephyr Cove, NV 89448 USA.

Color versions of one or more of the figures in this letter are available online at <http://ieeexplore.ieee.org>.

Digital Object Identifier 10.1109/LPT.2008.2008197

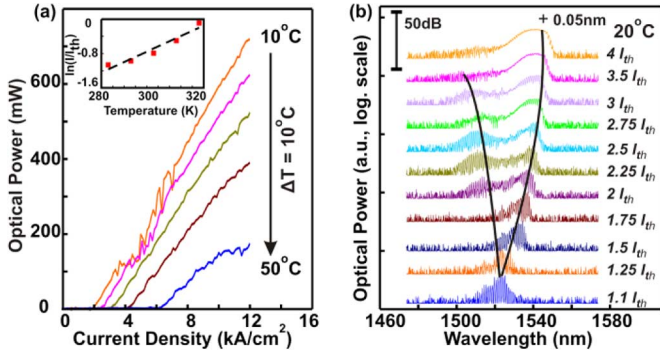


Fig. 1. (a)  $L$ - $I$  characteristics of the  $50 \times 300 \mu\text{m}^2$  broad-area Qdash laser at different temperatures. Up to  $\sim 450$ -mW total output power (from both facets) has been measured at  $J = 4.0 \times J_{\text{th}}$  at  $20^\circ\text{C}$ . (b) Progressive change of lasing spectra above threshold condition.

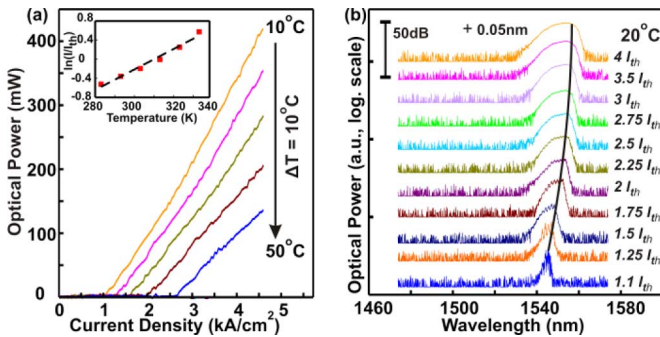


Fig. 2. (a)  $L$ - $I$  characteristics of the  $50 \times 1000 \mu\text{m}^2$  broad-area Qdash laser at different temperatures. Up to  $\sim 340$ -mW total output power (from both facets) has been measured at  $J = 4.0 \times J_{\text{th}}$  at  $20^\circ\text{C}$ . (b) Progressive change of lasing spectra above threshold condition.

samples into bars with different cavity lengths, the noncoated facet lasers were tested on a temperature controlled heat sink at  $20^\circ\text{C}$  with the epitaxial p-side-up mounting configuration. Current injection was performed under pulsed operation at 0.2% duty cycle with a  $2\text{-}\mu\text{s}$  pulsewidth.

### III. RESULTS AND DISCUSSION

Broad-area laser characterization provides evidence of emission from multiple sizes of Qdash ensembles as shown in Figs. 1 and 2 for fabricated lasers with different cavity lengths. The localized active region of the device can be treated as a large number of QD or Qdash, which can be further treated as a broad distribution of discrete energy levels [4]. This is owed to the inhomogeneous broadening nature of Qdash ensembles and the dash variation from different dash stacks. The light-current ( $L$ - $I$ ) curve of the short cavity Qdash laser ( $L = 300 \mu\text{m}$ ) yields a current density ( $J_{\text{th}}$ ) and slope efficiency of  $2.3 \text{ kA/cm}^2$  and  $0.46 \text{ W/A}$ , respectively [Fig. 1(a)]. Measuring the temperature-dependent  $J_{\text{th}}$  over a range of  $10^\circ\text{C}$ - $50^\circ\text{C}$ , reveals the temperature characteristic ( $T_o$ ) of  $41.3 \text{ K}$ . On the other hand, a long cavity Qdash laser ( $L = 1000 \mu\text{m}$ ) [Fig. 2(a)] yields  $J_{\text{th}} = 1.18 \text{ kA/cm}^2$ , slope efficiency of  $0.215 \text{ W/A}$ , and  $T_o$  of  $46.7 \text{ K}$  over the same temperature range. Compared to the laser with long cavity, the shorter cavity laser exhibits the progressive appearance of short wavelength emission line with an increase in injection level. The  $L$ - $I$  curve of the short cavity laser

shows kinks as compared to the long cavity laser. The jagged  $L$ - $I$  curve below  $\sim 3 \times J_{\text{th}}$  implies that the lasing actions from different confined energy levels are not stable due to the occurrence of energy exchange between short and long wavelength lasing modes [7], as can be seen in the lasing spectra of Fig. 1(b). In addition, the observation of kink for device tested at low temperature might also be a result of mode competition in the gain-guided, broad-area cavity devices. The calculated Fabry-Pérot mode spacing of  $\sim 1.1 \text{ nm}$  is well resolved in the measurement across the lasing wavelength span at low injection before a quasi-supercontinuum lasing is achieved, where the spectral ripple  $< 1 \text{ dB}$ . Subsequent injections contribute to the stimulated emission from longer wavelength or lower order subband energies while suppressing higher order subbands as shown in Fig. 1(b). This Qdash laser behavior is fundamentally different from the experimental observation from QD lasers with short cavity length, where the gain of lower subband is too small to compensate for the total loss, and lasing proceeds via the higher order subbands [8]. In Qdash laser, the initial lasing peak at shorter wavelength ( $\sim 1525 \text{ nm}$ ) is dominantly emitted from different groups of smaller size Qdash ensembles instead of higher order subbands of Qdash. Hence, the significant difference of  $\sim 11 \text{ meV}$  as compared to the dominant lasing peak of  $\sim 1546 \text{ nm}$  at high injection will contribute to photon reabsorption by larger size Qdash ensembles and seize the lasing actions at shorter wavelength. Regardless, a smooth  $L$ - $I$  curve at the injection above  $3 \times J_{\text{th}}$  due to the only dominant lasing modes at long wavelength demonstrates the high modal gain of the Qdash active core [1]. These observations indicate that carriers are easily overflows to higher order subbands because of the large cavity loss and the small optical gain [3] at moderate injection. At high injection, carrier emission time becomes shorter, when equilibrium carrier distribution is reached and lasing actions from multiple Qdash ensembles is seized [4].

A relatively smooth  $L$ - $I$  curve above the threshold is observed from the long cavity Qdash laser at all injection levels. The corresponding electroluminescence spectra show only one dominant peak emission at long wavelengths, unlike the short cavity Qdash lasers. This can be attributed to the effect of the long cavity parameter that results in smaller loss as compared to short cavity Qdash devices. The progressive redshift ( $\sim 10 \text{ nm}$ ) of lasing peak with increasing injection up to  $J = 4 \times J_{\text{th}}$  and the insignificant observation of band filling effect indicates that photon reabsorption occurs due to the photon-carrier coupling between different sizes of Qdash ensembles in addition to the high modal gain of the Qdash active core [1]. Injection above  $J = 4 \times J_{\text{th}}$  is expected to contribute to broader lasing span at long wavelength due to the high modal gain characteristics [1] although the comparison scheme of the two devices with different cavity lengths may not be fair without applying threshold current density.

Distinctive lasing lines are observed from different cavity Qdash lasers at the near-threshold injection of  $J = 1.1 \times J_{\text{th}}$ . The similarity of lasing wavelength (inset of Fig. 3) from devices with different cavity lengths further shows promise that the Qdash structures have high modal gain characteristics [1]. However, the Qdash laser with increasing cavity length shows

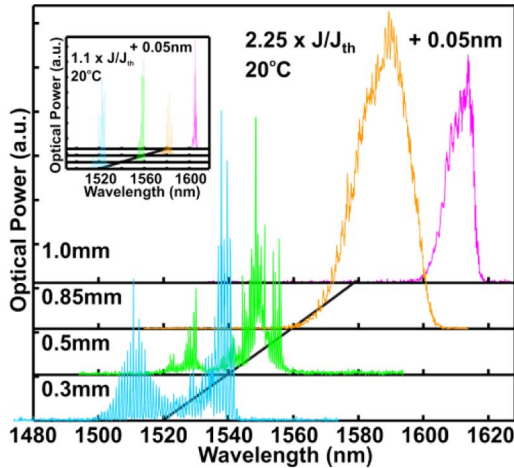


Fig. 3. Presence of different lasing Qdash ensembles with cavity length at the injection of  $J = 2.25 \times J_{th}$ . The inset shows the progressive redshift of lasing peak emission with cavity length at the injection of  $J = 1.1 \times J_{th}$ .

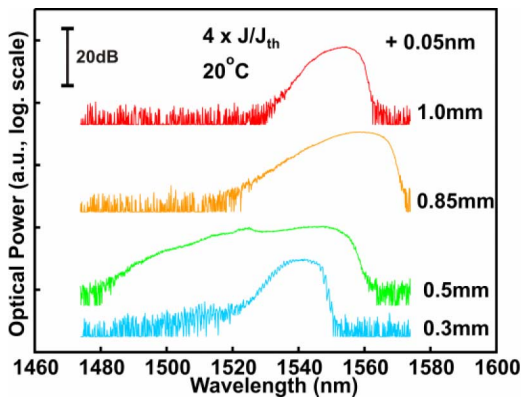


Fig. 4. Effect of cavity dependent on supercontinuum broadband emission from Qdash laser at the injection of  $J = 4 \times J_{th}$ .

progressive redshift (total of  $\sim 20$  nm up to  $L = 1000 \mu\text{m}$ ) of peak emission. This may be ascribed to the wide distribution of energy levels because of highly inhomogeneous broadening and photon reabsorption among Qdash families. At the intermediate injection of  $J = 2.25 \times J_{th}$ , simultaneous two-state laser emission, which is attributed to two groups of Qdash ensembles as mentioned previously, is noticed from short cavity Qdash lasers. On the other hand, a broad linewidth laser emission from a single dominant wavelength is shown in longer cavity Qdash lasers of 850 and  $1000 \mu\text{m}$  [Fig. 3]. The simultaneous two distinctive lasing peaks indicates localized three-dimensional energy level quantification in Qdash lasers as observed in QD lasers [8]. As a result, a supercontinuum broad laser emission could be achieved at high injection [Fig. 4]. An ultrabroad supercontinuum lasing bandwidth from devices with  $L = 500 \mu\text{m}$  results from emission in different order of energy subbands and groups of ensemble.

The broad lasing spectra from devices with different  $L$  suggest there is collective lasing from Qdashes with different ge-

ometries. However, the broad laser spectra of Qdash lasers obtained at room temperature are different from that of QD lasers which shows similar phenomenon but occur at low temperature below 100 K [3], [4]. In QD lasers, with increasing temperature, carriers can be thermally activated outside the dot into the well and/or barrier and then relax into a different dot [9]. Carrier hopping between QD states can favor a drift of carriers towards the dots where the lasing action preferentially takes place, thus resulting in a narrowing of the laser mode distribution. However, in Qdash lasers, carriers will be more easily trapped in the dash ensembles due to the elongated dimension in addition to random height distribution in each ensemble. These profiles of energy potential will support more carriers, thus retarding the emission of carriers [4] and resulting in a smaller homogeneous broadening at each transition energy level [9]. Hence, the actual carrier distribution in Qdash structures will be at high nonequilibrium and lead to supercontinuum lasing even at room temperature.

#### IV. CONCLUSION

Laser emission from multiple groups of Qdash ensembles instead of multiple orders of subband energy levels within a single Qdash ensemble has been experimentally shown. The suppression of laser emission in short wavelength and the progressive redshift of peak emission with injection from devices with short cavity length indicate the occurrence of photon reabsorption or energy exchange among different sizes of Qdash ensembles.

#### ACKNOWLEDGMENT

The authors would like to acknowledge IQE Inc. for the epitaxial growth of the Qdash samples.

#### REFERENCES

- [1] F. Lelarge, B. Dagens, J. Renaudier, R. Brenot, and A. Accard *et al.*, "Recent advances on InAs/InP quantum dash based semiconductor lasers and optical amplifiers operating at  $1.55 \mu\text{m}$ ," *IEEE J. Sel. Topics Quantum Electron.*, vol. 13, no. 1, pp. 111–124, Jan./Feb. 2007.
- [2] L. Harris, D. J. Mowbray, M. S. Skolnick, M. Hopkinson, and G. Hill, "Emission spectra and mode structure of InAs/GaAs self-organized quantum dot lasers," *Appl. Phys. Lett.*, vol. 73, pp. 969–971, 1998.
- [3] H. Shoji, Y. Nakata, K. Mukai, Y. Sugiyama, M. Sugawara, N. Yokoyama, and H. Ishikawa, "Lasing characteristics of self-formed quantum-dot lasers with multistacked dot layer," *IEEE J. Sel. Topics Quantum Electron.*, vol. 3, no. 2, pp. 188–195, Apr. 1997.
- [4] H. Jiang and J. Singh, "Nonequilibrium distribution in quantum dots lasers and influence on laser spectral output," *J. Appl. Phys.*, vol. 85, pp. 7438–7442, 1999.
- [5] H. S. Djie *et al.*, "Ultrabroad stimulated emission from quantum-dash laser," *Appl. Phys. Lett.*, vol. 91, no. 111116, pp. 1–3, 2007.
- [6] C. Xing and E. A. Avrutin, "Multimode spectra and active mode locking potential of quantum dot lasers," *J. Appl. Phys.*, vol. 97, no. 104301, pp. 1–9, 2005.
- [7] D. Hadass *et al.*, "Spectrally resolved dynamics of inhomogeneously broadened gain in InAs/InP 1550 nm quantum-dash lasers," *Appl. Phys. Lett.*, vol. 85, pp. 5505–5507, 2004.
- [8] A. Markus *et al.*, "Simultaneous two-state lasing in quantum-dot lasers," *Appl. Phys. Lett.*, vol. 82, pp. 1818–1820, 2003.
- [9] C. L. Tan, Y. Wang, H. S. Djie, and B. S. Ooi, "Role of optical gain broadening in the broadband semiconductor quantum-dot laser," *Appl. Phys. Lett.*, vol. 91, no. 061117, pp. 1–3, 2007.